On the Mixing of Protein Crystallization Cocktails

ARTICLE *in* CRYSTAL GROWTH & DESIGN · JUNE 2009

Impact Factor: 4.89 · DOI: 10.1021/cg801352d

CRYSTAL GROWTH & DESIGN
2009
VOL. 9, NO. 6
2707–2712

On the Mixing of Protein Crystallization Cocktails

Eduardo I. Howard,[†] José Miguel Fernandez,[‡] and Juan Manuel Garcia-Ruiz*[,§]

Instituto de Física de Líquidos y Sistemas Biológicos, CONICET-UNLP, c/ 59 no. 789 1900-La Plata, Argentina, Facultad de Medicina, Universidad de Granada, Avenida Madrid no. 11, E-18071 Granada, Spain, and Laboratorio de Estudios Crystalográficos, Instituto Andaluz de Ciencias de la Tierra, CSIC-Universidad de Granada, Edf. López Neyra, Avenida del Conocimiento, 18100-Armilla, Granada, Spain

Received December 13, 2008; Revised Manuscript Received March 21, 2009

Ⓜ This paper contains enhanced objects available on the Internet at http://pubs.acs.org/crystal.

ABSTRACT: The first step in the implementation of protein crystallization experiments by batch and vapor diffusion techniques is the mixing of the solution of the protein and the solution of the precipitating agent to form a drop. It is demonstrated by optical microscopy and by Mach−Zhender interferometry that, depending on the relative values of the properties of both solutions and on the sequence of mixing (protein over precipitant solution or vice versa), complex but well-defined fluid patterns occur. The formation of these patterns is governed by phenomena such as density-driven flow, Rayleigh−Taylor instability, diffusion reaction, and double-diffusive instabilities (both salt fingering and layering). The formation of local supersaturation maxima and minima in the crystallization drop due to these phenomena explains why and how the protocol of mixing may affect the crystallization results. As a practical application derived from this study, it is recommended that one perform active mixing when seeking reproducibility and avoid active mixing when seeking a more complex and extensive screening of the crystallization space.

Introduction

The crystallization of proteins is commonly performed by modifying their solubility in water with a solubility reductor, currently named a precipitating agent, which is in most cases either a salt (some of those salts categorized by Hoffmeister in his pioneering paper[1,2]) or a polymer (such as polyethylene glycol[3]). In practice, the solution of protein and the solution of the salt or polymer are mixed to form a crystallizing drop (batch technique) that in most cases is allowed to evaporate slowly until equilibrating with a reservoir containing a solution of the precipitating agent at higher concentration (vapor diffusion technique).[4,5] Thus, mixing is the first step for classical protein crystallization methods. It is currently assumed that the mixing process is instantaneous, and consequently, it is considered that the parameters relevant to crystallization (supersaturation, pH, etc.) vary at once in the whole volume of the drop. However, the mixture of these two liquids is not instantaneous, and therefore, the chemical conditions in a microliter-sized drop cannot be considered homogeneous. Actually, the precipitating agent and protein solutions have different values of physical properties such as density, viscosity, and surface tension, the values of which depend on concentration. In addition, the macromolecule and the precipitants have different values of diffusivity, particularly when saline solutions are used to reduce the solubility of the protein. Thus, it can be expected that the mixing would depend on (a) the relative properties of the protein and precipitant solution, (b) the type of mixing (slow addition of one solution to the other or active mixing), and (c) the sequence of mixing (protein solution over precipitant solution or vice versa).

The importance of the protocol of mixing has been pointed out in laboratory tips on protein crystallization,[6,7] but surprisingly little attention has been paid to study the elementary physics behind that mixing step.[8,9] This problem of mixing is of increasing interest in protein crystallization because of the recent trend to speed up the implementation of crystallization experiments in the framework of high throughput structural genomics. These large-scale projects make use of robotic crystallization stations that, in most cases, are based on classical drop techniques that require the mixing of the protein and precipitating solutions.[10–15] Reproducibility of the experiments[16,17] and scale up for crystal quality optimization are the two main problems related to the use of crystallization robots, clearly depending on the understanding and control of the mixing protocol.

In this paper, we present a study of the mixing behavior of a model protein solution (hen egg white lysozyme) with a solution of the salt (NaCl) commonly used to crystallize it. The study has been designed to cover the whole-phase diagram currently explored during screening for crystallization conditions. The experimental study has been performed by bright field and dark field optical microscopy and by Mach−Zhender interferometry. It is shown that complex but specific patterns are formed in this nonlinear system with a large number of degrees of freedom. We show that phenomena such as density-driven flow, Rayleigh−Taylor instability, diffusion reaction, and double-diffusive instabilities explain all of the experimental results. We found a correlation between the interpretation of the mixing experiments and the experimental results in terms of protein crystallization. Applications of the problem of mixing to crystallization robotics are discussed and suggestions for laboratory practice are offered.

Experimental Section

Protein solutions at different concentrations were prepared by dissolving hen egg white lysozyme purchased from Sigma (L6876, lot # 093k1455) without further purification in twice distilled water buffered at pH 4.5 with acetate solution 50 mM. Sodium chloride was purchased from Sigma (S7653, lot # 122k0078) and its solutions prepared also with twice distilled water. All of the experiments were performed twice,

* To whom correspondence should be addressed. Laboratorio de Estudios Crystalográficos, Edifício BIC Granada, Avenida de la Innovación, 1; P.T. Ciencias de la Salud. E-18100 Armilla, Granada, Spain. Tel: +34 958 750596. Fax: +34 958 750597. E-mail: jmgruiz@ugr.es.
[†] CONICET-UNLP.
[‡] Universidad de Granada.
[§] CSIC-Universidad de Granada.

10.1021/cg801352d CCC: $40.75
Published on Web 04/17/2009

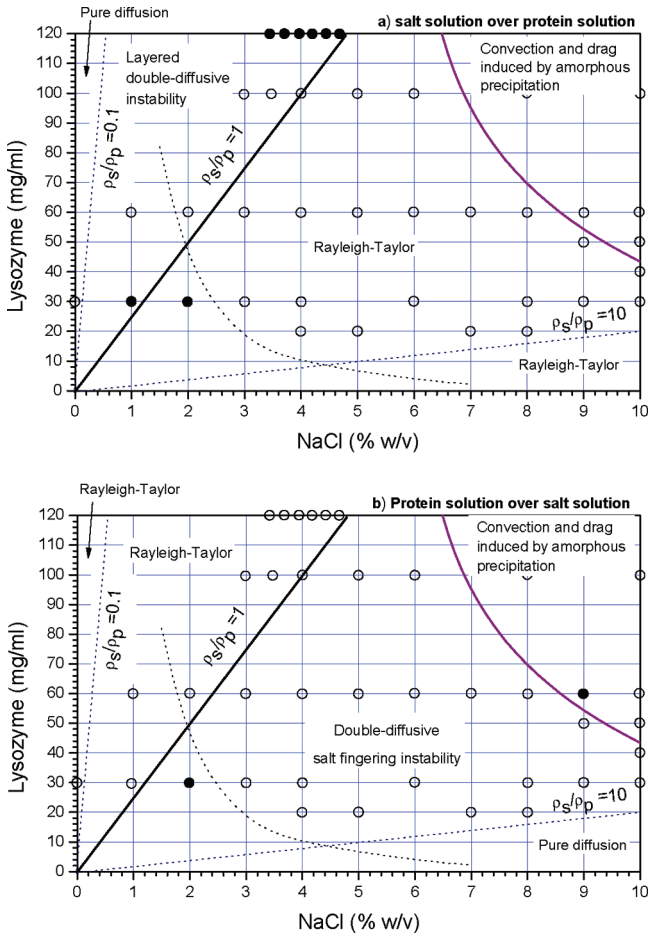

Figure 1. Protein solubility plots showing the isodensity line for lysozyme/NaCl solutions and the location of the mixing experiments carried out in this study. Experimental cases described in the text are labeled as filled circles. The plots show the mixing behavior for experiments performed (a) when the salt solution is poured over the protein solution and (b) when the protein solution is poured over the salt solution.

one pouring the sodium chloride solution on the protein solution and another one reversing the pouring sequence. These mixing experiments were recorded interferometrically to study the development on time of the fluid transport dynamics after mixing. The mixing was performed in a Hele-Shaw[18] type cell made of two parallel glass plates separated by a rubber spacer. The internal dimensions of the Hele-Shaw cell were 10 mm in height, 5 mm in width, and 0.9 mm in depth. Different concentrations of lysozyme solutions ranging from 30 to 120 mg/mL and NaCl solutions ranging from 0% to 10% were used (Figure 1). The first solution was poured into the cell carefully to avoid wetting the upper part of the glass walls of the cell. Then, the second solution was poured with a micropipet over the previous solution, slowly along the wall and avoiding bubbles. The Hele-Shaw cell was located in a Mach−Zhender interferometer described in ref 19. All of the experiments were performed at 20 ± 1 °C in a thermostated room.

An additional run of experiments was carried out to observe the crystallization behavior in larger solution volumes. The experiments were carried out in a 384-well plate. The radius of the wells was 3.8 mm, and the wells were filled with 50 μL of solution up to a height of 3.46 mm. These experiments were repeated three times, two as described above (direct and reverse mixing sequence) and another one by active mixing as performed usually in protein crystallization (aspirating and dispensing the drop in the pipet tip a few times). To reduce evaporation during the experimental time, the solutions were covered with mineral oil (Sigma M3516).

Results and Discussion

Figure 1 shows the Ostwald−Myers diagram of the dependence of the solubility of hen egg white lysozyme with respect to sodium chloride concentration. The diagram also includes the line of isodensity, which is the *loci* of the points where the density of the solutions of lysozyme (ρ_p) and NaCl (ρ_s) are equal. Any mixing experiment on the left of the isodensity line means that the lysozyme solution is denser than the NaCl solution, and any mixing experiment on the right of that line means that the lysozyme solution is lighter than the NaCl solution. A large number of mixing experiments were performed as shown in Figure 1. The main results relevant to the crystallization problem can be described by a few of these experiments showing characteristic patterns of well-known fluid dynamics behavior. Thus, we will describe only four selected representative experimental conditions using 30 mg/mL solutions of lysozyme and 1% and 2% solutions of NaCl, and 60 mg/mL lysozyme and 9% NaCl. In Figure 1 and everywhere in this paper, concentrations values refer to the initial concentration of the solutions before mixing, because these are the values relevant for the analysis of the result. This has to be noted because, typically, when batch or vapor diffusion experiments on protein crystallization are reported in the literature, concentration is given in values obtained after mixing.

Case 1: 1% Solution of NaCl Poured onto a 30 mg/mL Solution of Lysozyme. As shown in Figure 1a, the salt solution is lighter than the protein solution. As seen from density considerations, the system should be stable and the homogenization of the mixed solutions should be reached by simple cross diffusion of protein and salt molecules. However, as shown in Figure 2a, the system behaves unstably. Once the two solutions are in contact, a sharp interface is formed. After a few seconds (22 s in the experiment shown in Figure 2a, but time values depend on concentrations), the interface is broken by the formation of vertical convective flow as the salt solution enters the lower protein solution. This is followed by diffusive flow parallel to the vertical convective lines and finally by the formation of convective cells that work until the whole solution becomes homogeneous. This behavior is due to a phenomenon known as layered double-diffusive instability[20,21] and it is schematically shown in Figure 2b. The instability is triggered by the difference in diffusivity between the two solutes, namely, the protein diffusion coefficient is 1 order of magnitude smaller than that of NaCl. At the interface, the salt molecules diffuse toward the lysozyme solution faster than the lysozyme molecules toward the salt solution. That makes the solution in the local volume below the interface enriched in salt but not largely depleted in lysozyme. The solution in that location becomes heavier and falls down as shown in Figure 2b. Conversely, by the same mechanism, the solution, which is close to the upper part of the interface, becomes lighter and flows up. The result is the formation of the layered double-diffusive convection that tends to increase the homogenization process. However, except pure diffusion, this phenomenon is slower than the ones operating in the next two cases.

Case 2: 2% Solution of NaCl Poured onto a 30 mg/mL Solution of Lysozyme. The next case shows how an increment of just 1% of NaCl concentration (from 1% to 2%) results in a drastically different mixing behavior. This is related to the fact that the 2% solution of salt now becomes denser than the 30 mg/mL protein solution. Consequently, after the solutions are poured, the system becomes gravitationally unstable and turbulent flow immediately appears. Even when the density ratio is close to one, a sharp interface may be formed, but this interface quickly breaks as small perturbations at the interface grow and the symmetry is broken, a phenomenon known as Rayleigh−Taylor instability.[22] The rate at which the mixing

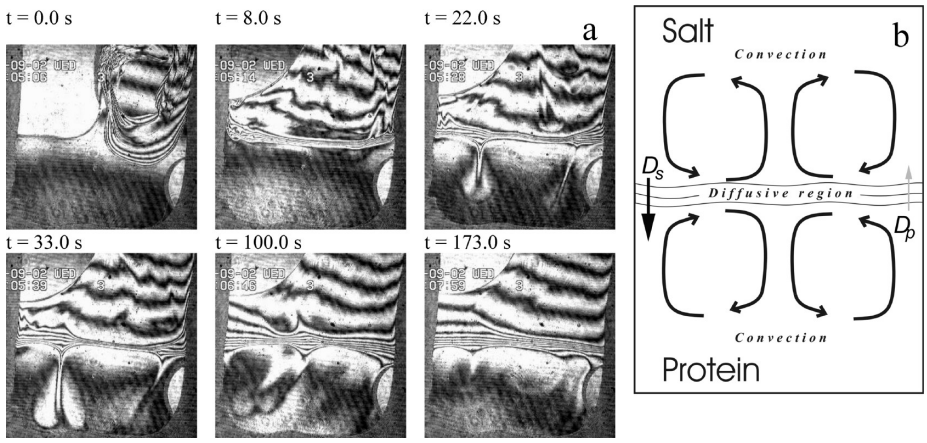

Figure 2. (a) Series of six frames selected from the interferometric video in WMV format (time scale, 2 frames/s) corresponding to the experiment described as case 1. (b) Explanation of the layered double-diffusive instability. The diffusivity of the protein molecules D_p toward the upper salt solution is slower than the diffusivity of the salt molecules D_s toward the lower protein solution. This triggers a convective mechanism that enhances mixing.

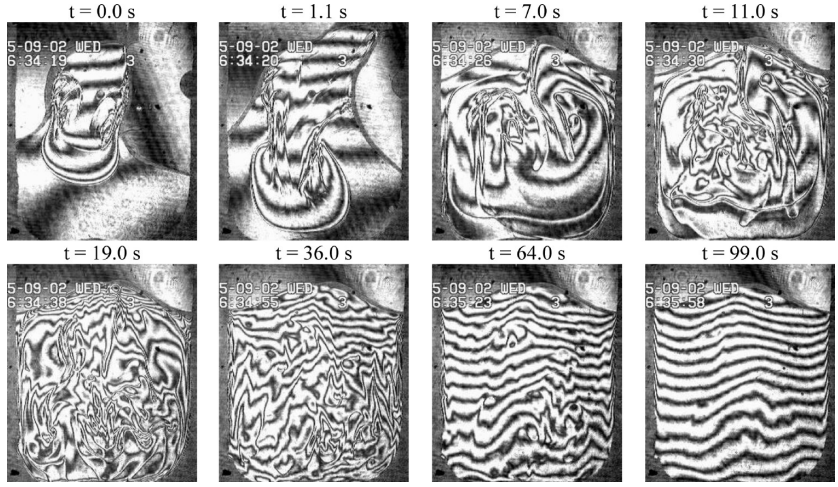

Figure 3. Series of frames selected from the interferometric video in WMV format (time scale, 2 frames/s) corresponding to the experiment described as case 2. Note that the system becomes turbulent as a result of the development of Rayleigh−Taylor instability, and the cocktail becomes homogeneous in less than 1min.

develops depends not only on the properties of solutions but also on pipetting and the cell's shape. As shown in the time sequence of interferograms in Figure 3, turbulent mixing allows homogenization in a few seconds, but a density layering may develop after that.

Case 3: 30 mg/mL Solution of Lysozyme Poured onto 2% Solution of NaCl. This is the same experiment as case 2 but reversing the mixing sequence, i.e., pouring the lighter 30 mg/mL protein solution onto the denser 2% NaCl solution. As seen from density considerations, the system should be stable. Consequently, as shown in Figure 4a, a sharp interface is created after the solutions are poured. However, a few seconds later (about 16 s in Figure 4a), before the interface becomes visibly thicker by pure diffusion, finger-shaped structures form. The origin of that fingering is schematically shown in Figure 4b and is again related to the difference in diffusivities between the salt and protein molecules. At the interface, some small stochastic pocket fluctuations form. In those pockets of protein solution inside the salt solution, the salt molecules quickly enter the pocket locally enriching the solution in NaCl while the pocket looses only a small amount of protein molecules. Those pockets become denser than the solution below them, acquiring unstable buoyancy and start to fall down. This is a self-feeding phenomenon, because as the pocket falls down forming a finger, its density and its rate of sedimentation increase. In parallel, pockets of NaCl solution inside the protein solution loose salt molecules quickly while the protein molecules enter slowly. This makes the solution in pocket lighter than the solution above it, and consequently, the pocket rises, forming a finger. This is the so-called double-diffusive salt fingering instability,[23,24] a well-known process in fluid dynamics. As shown in Figure 4a, the mixing due to the existence of this instability makes the solution homogeneous in a couple of minutes.

Case 4: 60 mg/mL Solution of Lysozyme Poured onto 9% Solution of NaCl. In this case, located at the right of the isodensity line $\rho_S/\rho_P = 1$, the phenomenon of double-diffusive salt fingering should also account for the phenomenology of mixing. However, at such high concentrations of salt, protein precipitation occurs at the interface forming solid particles either amorphous or crystalline that are heavier than the liquid below, and therefore, they tend to sediment according to Stokes law. As shown in Figure 5, a sharp interface is formed and the particles start to nucleate and grow; the waiting time to nucleation is a function of the initial concentrations, which in turn depends on the rate of diffusive mixing at the interface.

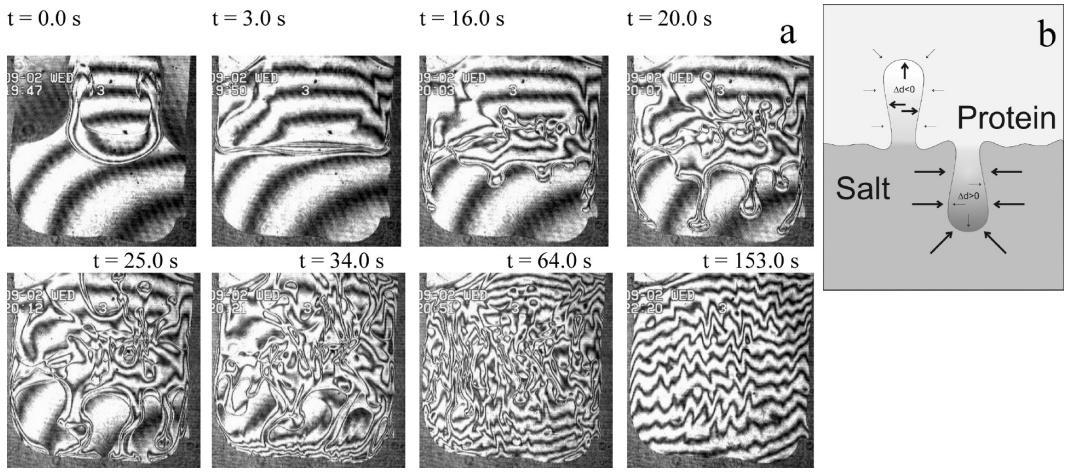

Figure 4. (a) Series of eight frames selected from the interferometric video corresponding to the experiment described as case 3. The phenomenon of double-diffusive salt fingering instability is clearly observed, which is schematically explained in (b). Note that salt molecules (thick arrows) diffuse faster into the pockets of proteins than the protein molecules (thin arrows) into the pockets of salts. That simple mechanism creates density differences between the pockets and the surrounding solution that provokes the formation of upward salt-rich fingers and downward protein-rich fingering. An interferometric video in WMV format (time scale, 2 frames/s) recording an experiment similar to that described as case 3 in the text, but with 30 mg/mL lysozyme protein solution over a 3% NaCl solution, is available as a WEO.

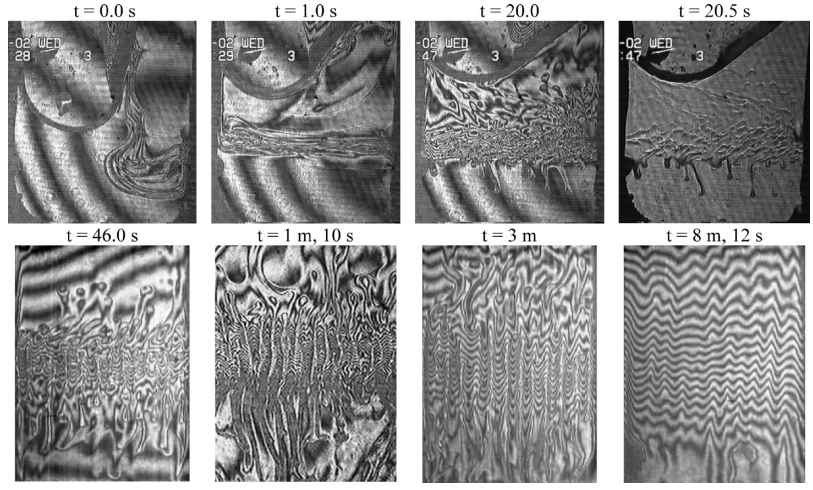

Figure 5. Series of frames corresponding to the experiment described as case 4. All of the frames were selected from the interferometric video in WMV format (time scale, 2 frames/s), except the fourth frame ($t = 20.5$ s), which was obtained by normal optical illumination. The interferometric mode switches to normal optical illumination between 27 and 34 s. Note that due to the high concentration of the solutions, the fluid is mixed by drag of the precipitated protein.

Table 1

	1 day		5 days	
[NaCl], % (w/v)	no mixing	mixing	no mixing	mixing
3.6	clear drop	clear drop	clear drop	clear drop
3.8	clear drop	clear drop	clear drop	clear drop
4.0	few isolated crystals	clear drop	few isolated crystals	clear drop
4.2	crystals	clear drop	crystals	clear drop
4.4	lots of crystals	clear drop	lots of crystals	few isolated crystals
4.6	lots of crystals	clear drop	lots of crystals	many crystals

When the particles are formed before salt fingering is triggered, their sedimentation dominates mixing. However, in some cases, perturbations at the interface by double-diffusive salt fingering instability appear before precipitation. Then, the fingers start to develop, but the concentration of salt inside them increases while the concentration of lysozyme remains practically constant. This is why precipitates can be observed to form while fingering falls down, which obviously modifies the mixing behavior. The existence of precipitation is clearly demonstrated when the experiment is observed by optical interferometry at 20 s (third frame of Figure 5) and optical microscopy at 20.5 s (fourth frame of Figure 5).

Discussion

According to the above results, the Ostwald−Myers diagram can be divided from the point of view of mixing in several regions as schematically shown in Figure 1. When the solution of salt is poured onto the lysozyme solution (Figure 1a), four regions can be distinguished. On the left on the isodensity region

($\rho_S/\rho_P = 1$), layered double-diffusive instability dominates until the line defined by $\rho_S/\rho_P \approx 0.1$, when the mechanisms of mixing start to be dominated by pure diffusion. On the right of the isodensity line, mixing occurs by turbulent buoyancy triggered by Rayleigh−Taylor instability. In the upper right corner for high concentration of both protein and salt, this turbulent mixing is accompanied by sedimentation of solid denser particles formed by precipitation or by oily drops formed by liquid−liquid demixing. When the protein solution is poured onto the salt solution, the mixing behavior changes, but it is not just reversed (Figure 1b) because another instability, double-diffusive salt fingering, appears. In fact, double-diffusive salt fingering dominates the mixing behavior from the isodensity line $\rho_S/\rho_P = 1$ to the line of $\rho_S/\rho_P \approx 10$, the values at which diffusion starts to account for mixing. On the left of the isodensity line, when the heavier lysozyme solution is located on top of the lighter salt solution, Rayleigh−Taylor instability and turbulent mixing account for the observed mixing history. Finally, at high concentration of protein and salt solution, a solid phase at the interface is formed which triggers sedimentation governed by Stokes drag law.

Each of the processes and instabilities of the stability maps shown in panels a and b of Figure 1 affect the mixing velocity and the waiting time for the solution to be considered homogeneous for practical purposes (i.e., for local supersaturation variation not affecting the waiting time for nucleation). As seen from the rate of mixing, the phenomena in the stability map can range from a low to high mixing rate as plain diffusion, layered double-diffusive instability, double-diffusive salt fingering, Rayleigh−Taylor, drag, and sedimentation. Certainly, the fastest way to homogenization is by active mixing, which is performed in protein crystallization by iterative pipetting. This mixing behavior might affect crystallization results when the transient states to homogenization provoke local values of supersaturation high enough to induce crystallization, amorphous precipitation, or liquid−liquid demixing. Nucleation kinetics is affected by the area and by the lifetime of the interface at the interface between the solutions,[25] which depends not only on the time for homogenization but also on mixing type. In fact, for all those cases in which the waiting time for homogenization is longer than the waiting time for nucleation, the mixing problem affects the crystallization results. In some cases, that effect can be difficult to measure. However, it can be easily visualized when the induction of precipitation is irreversible or at least is powerful enough to be observed by optical microscopy. This is what we demonstrate with the crystallization experiment accompanying this mixing study. We selected the mixing of a lysozyme solution of 120 mg/mL and a buffered water solution of sodium chloride from a concentration of 3.6−4.6%. These concentration values might appear too high, but it must be remembered that the final conditions after homogenization are 60 mg/mL lysozyme and 1.8−2.5% NaCl, which are conditions reported to grow tetragonal lysozyme in the laboratory.[26] After homogenization, these concentrations yield supersaturation values inside the crystallization metastable zone in the range of C/Ce = 1.0−2.0. However, at the interface between the two solutions, the supersaturation value ranges between 8.6 and 13.6. Two types of experiments were performed. In the first one, the protein solution was located in the well and the salt solution was carefully poured on it to avoid active mixing. In the second one, the solutions were actively mixed with the pipet and homogenization occurred immediately. In the first one, according to Figure 1a, it is expected to have layered double-diffusive instability. As shown in Table 1, the differences are clear. In most cases, we observed differences in waiting times for nucleation, number, and size of crystals, as well as in crystal distribution. In some cases, as for instance that corresponding to a NaCl concentration of 4.2% (w/v), the results are so dramatic that, depending on performing active mixing or not, either tens of crystals or just a clear drop can be obtained.

All of the experiments reported in this study have been performed with hen egg white lysozyme. Lysozyme is a model protein for crystallization studies with a rather low molecular weight (14 600 D). Note that the observed effects of mixing will be larger for proteins of higher molecular weight, and therefore our results are significant, because they can be extrapolated for most protein crystallization studies, particularly for large macromolecular complexes. The experimental setup of our experiments is similar to that of batch experiments or sitting drop experiments. In the case of hanging drop experiments, the drop is reverted with respect to gravity and this introduces a new variable. However, if the time elapsed since the drop is made until it is reversed is longer than the longest mixing time, all of the results found in our experiments are as valid as for the cases of batch methods and sitting drop methods. Our results explain why two vapor diffusion experiments or two batch experiments performed with identical chemical composition of the protein and precipitant solutions can yield different results, an observation that has puzzled the crystallization community for years. It is also important to emphasize that the way in which protein and precipitant solutions mix depends on the characteristic length of the experiment, i.e., on the size of the drop, because it increases the ratio between convective and diffusive mass transport, i.e., the Rayleigh number. In particular, it must be expected that different crystallization occurs when one scales-up screening experiments performed with drops of tens of nanoliters to the microliter scale. Finally, our results also underline the differences between performing screening with vapor diffusion and batch techniques (i.e., drop techniques) and counterdiffusion and other techniques that use liquid−liquid mixing in thin capillary volumes or gelled solutions. In the last case, the mixing occurs purely by diffusion mass transport and the screening of the crystallization space is wider and occurs with a different kinetics.[27] Actually, drop techniques will also behave differently when convection is removed, i.e., when experiments are performed in actual microgravity,[28] gel,[29] and a strong magnetic field.[30,31]

Conclusions

The study of the mixing of precipitant and protein solutions by optical microscopy and Mach−Zhender interferometry reveals a number of phenomena taking place at the interface between the two solutions. These phenomena, mostly physical instabilities, affect the waiting time for homogenization and the precipitation behavior, and they may affect in many practical cases the results of the crystallization experiment. The triggering of the fluid physics instabilities is related to the different physical properties of the precipitating agent and protein solutions, including density, viscosity, and surface tension (which are properties that are known to depend on concentration) and diffusivity. A number of suggestions can be made for practical purposes. To add the higher density solution over the less dense one is a good option, if one looks for spontaneous homogenization since that combination will follow turbulent mixing and the Rayleigh−Taylor instability pattern. However, when we look for the maximum number of nuclei, exploring the reverse condition could be interesting because fingering or layering may

enhance nucleation along the evolving interfaces created by fluid dynamics. Finally, an obvious alternative is active mixing. Working manually, it is possible and easy to mix the solutions actively, but it is not trivial to incorporate a good mixing step in the automated, high-throughput oriented, crystallization devices.

As a practical corollary of the results, it is recommended that one perform mixing when seeking reproducibility and avoid mixing when seeking a more complex and extensive screening of the crystallization space.

Acknowledgment. We gratefully acknowledge Ignacio Vico for his technical help with the interferometer and A. A. Bianchi (Servicio de Hidrografía Naval, Argentina), Diego Vallejo (Universidad de La Plata, Argentina), and Dr. José Gavira (CSIC-Universidad de Granada) for useful discussions. Financial support was provided by Plan Propio, Universidad de Granada, Spain. E.I.H is a member of the Carrera del Investigador Conicet-Argentina. This paper is a product of the Factoría de Crystalización, a Consolider-Ingenio 2010 project of the Spanish Ministerio de Eduación y Ciencia.

References

(1) Hofmeister, F. *Arch. Exp. Pathol. Pharmakol.* **1888**, *24*, 247–260. Translated in: Kunz, W.; Henle, J.; Ninham, B. W. *Curr. Opin. Colloid Interface Sci.* **2004**, *9*, 19–37 doi: 10.1016/j.cocis.2004.05.005.

(2) Riès-Kautt, M.; Ducruix, A. F. *J. Cryst. Growth* **1991**, *110*, 20–25 doi: 10.1016/0022-0248(91)90861-X.

(3) Kulkarni, A. M.; Chatterjee, A. P.; Schweizer, K. S.; Zukoski, C. F. *J. Chem. Phys.* **2000**, *113*, 9863–9873 doi: 10.1063/1.1321042.

(4) Ducruix, A., Giegé, R., Eds. *Crystallization of nucleic acids and proteins: a practical approach*; Oxford University Press: Oxford, 1999; pp 149−175; ISBN 0-19-963678-8.

(5) McPherson, A. *Crystallization of Biological Macromolecules*; Cold Spring Harbor Laboratory Press: New York, 1999; ISBN 0-87969-617-6.

(6) http://www.hamptonresearch.com/support/gentips.html.

(7) http://xray.bmc.uu.se/~terese/index.html.

(8) Chernov, A. A. *J. Struct. Biol.* **2003**, *142*, 3–21 doi: 10.1016/S1047-8477(03)00034-0.

(9) Lima, D.; De Wit, A. *Phys. Rev. E* **2004**, *70*, 021603–7 doi: 10.1103/PhysRevE.70.021603.

(10) Cox, M. C.; Weber, P. C. *J. Appl. Crystallogr.* **1987**, *20*, 366–373 doi: 10.1107/S0021889887086461.

(11) Stevens, R. C. *Curr. Opin. Struct. Biol.* **2000**, *10*, 558–563 doi: 10.1016/S0959-440X(00)00131-7.

(12) Mueller, U.; Nyarsik, L.; Horn, M.; Rauth, H.; Przewieslik, T.; Saenger, W.; Lehrach, H.; Eickhoff, H. *J. Biotechnol.* **2001**, *85*, 7–14 doi: 10.1016/S0168-1656(00)00349-7.

(13) Luft, J. R.Wolfley, J. Jurisica, I.Glasgow, J. Fortier, S. DeTitta, G. T. *J. Cryst. Growth* **2001**, *232*, 591–595 doi: 10.1016/S0022-0248(01)01206-4.

(14) Krupka, H. I. Rupp, B. Segelke, B. W. Lekin, T. P. Wright, D. Wu, H.-C. Todd, P. Azarani, A. *Acta Crystallogr.* **2002**, *D58*, 1523–1526 doi: 10.1107/S090744490201435X.

(15) Eisenstein, M. *Nature Methods* **2007**, *4*, 95–102 doi: 10.1038/nmeth0107-95.

(16) Newman, J. Xu, J. Willis, M. C. *Acta Crystallogr.* **2007**, *D63*, 826–832 doi: 10.1107/S0907444907025784.

(17) Wooh, J. W. Kidd, R. D. Martin, J. L. Kobe, B. *Acta Crystallogr.* **2003**, *D59*, 769–772 doi: 10.1107/S0907444903002919.

(18) Hele-Shaw, H. S. *Nature (London, U.K.)* **1898**, *58*, 33–36 doi: 10.1038/058034a0.

(19) García-Ruiz, J. M. Novella, M. L. Otálora, F. *J. Cryst. Growth* **1999**, *196*, 703–710 doi: 10.1016/S0022-0248(98)00851-3.

(20) Turner, J. S. Ed. *Buoyancy Effects in Fluids*; Cambridge University Press: Cambridge, U.K., 1980; ISBN 0521297265.

(21) Ruddick, B. Gargett, A. E. *Prog. Oceanogr.* **2003**, *56*, 381–393 doi: 10.1016/S0079-6611(03)00024-7.

(22) Taylor, G. I. *Proc. R. Soc. London* **1950**, *A 201*, 192–196 doi: 10.1098/rspa.1950.0052.

(23) Schmitt, R. W., Jr. *Sci. Am.* **1995**, *272* (5), 70–75.

(24) Pringle, S. E. Glass, R. J. Cooper, C. A. *Transp. Porous Media* **2002**, *47*, 195–214 doi: 10.1023/A:1015535214283.

(25) Chen, D. L. Gerdts, C. J. Ismagilov, R. F. *J. Am. Chem. Soc.* **2005**, *127*, 9672–9673 doi: 10.1021/ja052279v.

(26) Pusey, M. Witherow, W. Naumann, R. *J. Cryst. Growth* **1988**, *90*, 105–111 doi: 10.1016/0022-0248(88)90304-1.

(27) Otálora, F.; García-Ruiz, J. M. *J. Cryst. Growth* **1996**, *169*, 361–367 doi:10.1016/S0022-0248(96)00394-6.

(28) Otálora, F. Novella, M. L.Gavira, J. A. Thomas, B. García-Ruiz, J. M. *Acta Crystallogr.* **2001**, *D57*, 412–417 doi: 10.1107/S0907444901000555.

(29) García-Ruiz, J. M. Novella, M. L. Moreno, R. Gavira, J. A. *J. Cryst. Growth* **2001**, *232*, 165–172 doi:10.1016/S0022-0248(01)01146-0.

(30) Poodt, P.; W, G.; Heijna, M. C. R.; Christianen, P. C. M.; van Enckevort, W. J. P.; de Grip, W. J.; Tsukamoto, K.; Maan, J. C.; Vlieg, E. *Cryst. Growth Des.* **2006**, *6*, 2275–2280 doi: 10.1021/cg0600546.

(31) Wakayama, N. I. *Cryst. Growth Des.* **2002**, *3*, 17–24 doi: 10.1021/cg025565g.

CG801352D